Bioorganic & Medicinal Chemistry xxx (2016) xxx–xxx

Contents lists available at ScienceDirect

Bioorganic & Medicinal Chemistry

journal homepage: www.elsevier.com/locate/bmc

Structure activity relationship studies on chemically non-reactive glycine sulfonamide inhibitors of diacylglycerol lipase

Louis S. Chupak [a,*], Xiaofan Zheng [a], Shuanghua Hu [a], Yazhong Huang [a], Min Ding [a], Martin A. Lewis [b], Ryan S. Westphal [b], Yuval Blat [c], Andrea McClure [d], Robert G. Gentles [a]

[a] Discovery Chemistry, Research and Development, Bristol-Myers Squibb Co., 5 Research Parkway, Wallingford, CT 06492, USA
[b] Neuroscience Biology, Disease Sciences and Biologics, Research and Development, Bristol-Myers Squibb Co., 5 Research Parkway, Wallingford, CT 06492, USA
[c] Lead Evaluation, Discovery, Research and Development, Bristol-Myers Squibb Co., 5 Research Parkway, Wallingford, CT 06492, USA
[d] Discovery Chemistry Platforms, Research and Development, Bristol-Myers Squibb Co., 5 Research Parkway, Wallingford, CT 06492, USA

ARTICLE INFO

Article history:
Received 4 December 2015
Revised 28 January 2016
Accepted 5 February 2016
Available online xxxx

Keywords:
Diacylglycerol
Lipase inhibitor
Endocannabinoid
2-Arachidonoylglycerol
Glycine
Sulfonamide

ABSTRACT

N-Benzylic-substituted glycine sulfonamides that reversibly inhibit diacylglycerol (DAG) lipases are reported. Detailed herein are the structure activity relationships, profiling characteristics and physicochemical properties for the first reported series of DAG lipase (DAGL) inhibitors that function without covalent attachment to the enzyme. Highly potent examples are presented that represent valuable tool compounds for studying DAGL inhibition and constitute important leads for future medicinal chemistry efforts.

1. Introduction

Regulation of the endocannabinoid signaling system is an emerging strategy for potential therapeutic intervention in a variety of diseases,[1] including; anxiety,[2] depression,[3] pain,[4] inflammation,[5] hepatic steatosis and obesity.[6] Here we describe efforts to regulate the endocannabinoid signaling system by modulating the levels of the endogenous cannabinoid agonist, 2-arachidonoylglycerol (2-AG) through inhibition of the enzymes predominantly responsible for its biosynthesis.

The endocannabinoid signaling system consists of the cannabinoid receptors CB_1 and CB_2, the endogenous agonists (endocannabinoids) anandamide (ANA) and 2-AG, and the enzymes that regulate endocannabinoid synthesis and degradation. CB_1 and CB_2 are G-protein coupled receptors (GPCRs) that are widely distributed throughout the body. CB_1 is one of the most abundant GPCRs in the brain and is also located to a lesser extent in the liver, adipose tissue, gastrointestinal tract, as well as in vagal nerves, pancreas and skeletal muscle. In contrast, CB_2 is found mainly in cells of the immune system.[7–12]

Attempts to prepare compounds that modulate the CB_1 or CB_2 receptors without inducing significant side effects have met with limited success. For example, the synthetic cannabinoid agonist nabilone is approved for the treatment of chemotherapy-induced nausea and vomiting that has not responded to conventional antiemetics. However, nabilone produces psychoactive side effects similar to those observed with marijuana.[13] The CB_1 antagonist rimonabant and the inverse agonist taranabant inhibit food intake and reduce body weight in obese animals and humans. However, these agents are known to induce central nervous system (CNS) side effects including anxiety and depression.[14]

An emerging alternative strategy to receptor agonism or antagonism is to regulate tissue levels of the endocannabinoids.[12,5,15] Presented here are the SAR, profiling properties and pharmacokinetics of the first reported chemically non-reactive inhibitors of 2-AG synthesis.[16,17] Diminished 2-AG levels are expected to produce a corresponding reduction in cannabinoid receptor (CR) activation. Unlike many typical neurotransmitters, 2-AG is not stored in vesicles; rather, it is rapidly synthesized (in an on-demand fashion) in response to rising cellular calcium levels, or alternatively, by activation of $G_{q/11}$ protein coupled receptors.[12,15,18,19] 2-AG is produced by the reaction sequences depicted in Figure 1.[20] Initial cleavage of the sugar moiety from membrane associated phosphatidyl inositol by phosphatidyl lipase C (PLC) results in the for-

* Corresponding author. Tel.: +1 203 677 7233.
E-mail address: louis.chupak@bms.com (L.S. Chupak).

http://dx.doi.org/10.1016/j.bmc.2016.02.006
0968-0896/

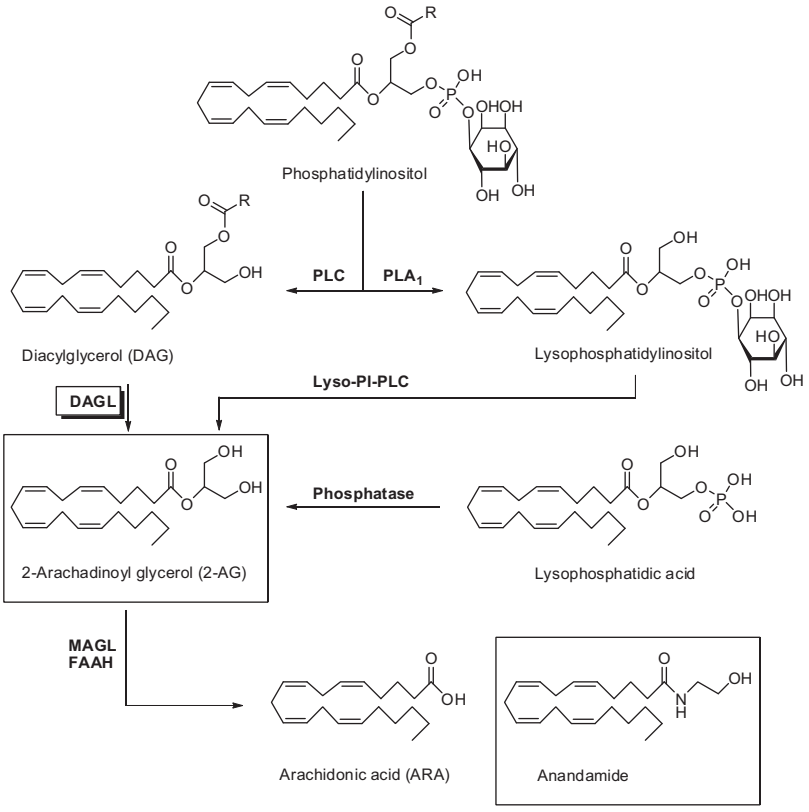

Figure 1. Principal endocannabinoids 2-AG and anandamide. The major routes for the anabolism and catabolism of 2-AG are shown. Enzymes exist to catalyze the reverse reactions depicted in most of the anabolic steps shown, and the transient tissue concentrations of 2-AG represent the balance between the rates of these competing reactions. Fatty acid amide hydrolaze (FAAH), phosphatidylinositol-specific phospholipase C (Lyso-PI-PLC), Phospholipase A1 (PLA_1).

mation of diacylglycerol (DAG). DAG is subsequently hydrolyzed by diacylglycerol lipase (DAGL) resulting in the formation of 2-AG. Once formed, 2-AG acts as a retrograde messenger by activating CRs on presynaptic neurons. Alternatively, 2-AG can be synthesized by the phosphatase mediated cleavage of lysophosphatidic acid, though this pathway is thought to be a minor contributor to tissue levels. In relation to its catabolism, 2-AG is cleared by the action of several enzymes, with the major pathway thought to involve monoacylglycerol lipase (MAGL). Thus the levels of 2-AG are tightly controlled primarily by the actions of DAGL and MAGL. Consistent with this observation is that genetically-modified animals that lack DAGL-α exhibit decreased tissue concentrations of 2-AG.[21,22]

In this manuscript, we focus on inhibiting the activity of DAGL as a point of potential therapeutic intervention. Inhibition of DAGL should lead to reduced levels of 2-AG and a corresponding reduction in CR activation.[23] Consequently, it is anticipated that a DAGL inhibitor will be functionally equivalent to a CR antagonist. However, the effects of a DAGL inhibitor would be localized to sites where 2-AG is actively being synthesized, and thus it might be anticipated to have an improved side-effect profile relative to a CR antagonist.

DAGLs are serine hydrolases that exist as membrane associated proteins. There are two known isoforms of the enzyme, DAGL-α and DAGL-β.[24] DAGL-α is predominantly found in the CNS where it is localized in post-synaptic neurons (Fig. 2), in contrast to DAGL-β that is found mainly in the periphery.[21,25,26] Postsynaptic neurons generate and release 2-AG which acts as a retrograde messenger by activating CRs on presynaptic neurons.[27,28] Activation of the presynaptic CR regulates the release of the neurotransmitters GABA and glutamate. In certain disease states, tissue levels of 2-AG can be altered and result in changes to the activation level of

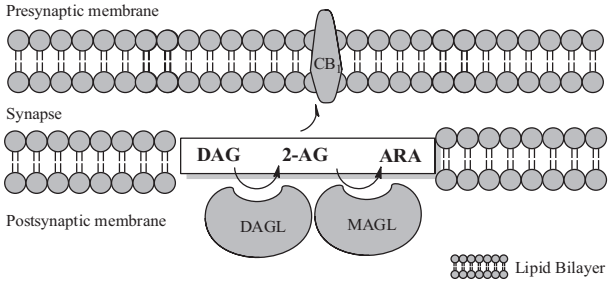

Figure 2. Sites of synthesis and degradation of 2-AG and a depiction of its role as a retrograde neurotransmitter; activation of presynaptic CB_1 receptors can result in a variety of responses dependent on the G-protein to which the receptor is coupled.

the CRs.[9–11,29–31] This activation can impact the functional output of the GABAergic and glutamatergic systems, as is the case in Alzheimer's or Parkinson's diseases where the regulatory function of 2-AG is thought to be disrupted.[29] 2-AG also functions in the periphery, where DAGL inhibitors are anticipated to have therapeutic potential in the treatment of diseases such as obesity, metabolic syndrome, liver fibrosis and allergic contact dermatitis.[5,10,11,32]

Prior to our initial disclosure[16,17] and a subsequent related publication,[25] the only reported inhibitors of DAGL were chemically reactive molecules that function by covalently modifying DAGL. Such irreversible inhibitors are expected to display several potential liabilities related to toxicity and a lack of selectivity. For example, tetrahydrolipstatin (**1**) covalently modifies both DAGL-α and DAGL-β (Fig. 3).[33] In addition, **1** blocks several brain serine hydrolases with similar potencies to those observed against DAGL-α and

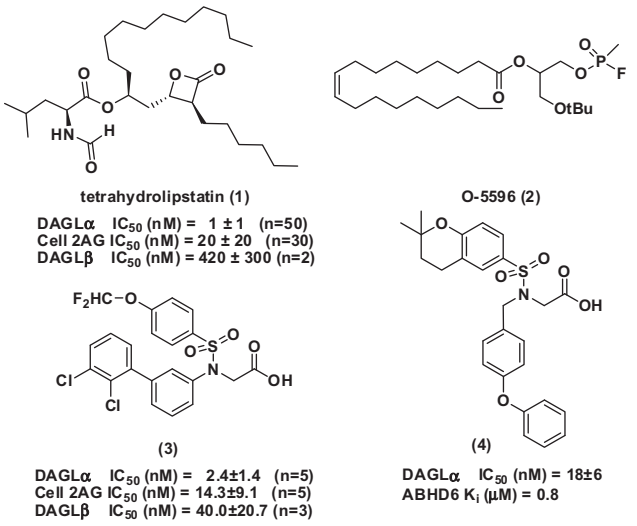

Figure 3. Reported inhibitors of DAGL.

DAGL-β.[34] More selective compounds have been reported: for example, **2** is an irreversible inhibitor of DAGL-α, but does not inhibit MAGL or fatty acid amide hydrolase, a key enzyme involved in the degradation of anandamide (see Fig. 1).[35] Compound **2** is not an antagonist of the CB_1 or CB_2 receptors, but shows effects that mimic CR antagonism. Intraperitoneal administration of **2** reduced mouse intake of palatable food consistent with a reduction in 2-AG levels. Thus, this compound has been shown to be valuable as both an in vitro and in vivo tool for studying 2-AG biosynthesis. However, the need remains for chemically non-reactive inhibitors of DAGL that might function as starting points for drug design.

To that end, our corporate compound file was screened for inhibitors of DAGL-α. A series of glycine sulfonamide derivatives was discovered and initial hit to lead optimization exercises resulted in the identification of 2-(*N*-(2′,3′-dichloro-[1,1′-biphenyl]-3-yl)-4-(difluoromethoxy)phenylsulfonamido)acetic acid (**3**), as an early lead compound, see Figure 3 (manuscript in preparation). This compound is an orally bioavailable, non-covalent inhibitor of both DAGL-α and DAGL-β, with IC_{50}s of 2.4 and 40 nM, respectively. Compound **3** was also shown to reduce 2-AG levels in a whole-cell assay (EC_{50} 14 nM) and was demonstrated to induce a reduction in 2-AG levels in liver tissue when dosed intraperitoneally (IP) in mice. Additionally, compound **3** did not inhibit MAGL at the highest tested concentrations of 30 μM.

Recently, the activity profiles of a related series of glycine sulfonamides were reported.[36] These compounds were derived from analogs of compound **3**[17] by introduction of an oxygen spacer to change the biaryl functional group into a biaryl ether. In selectivity studies, compound **4**[25] was shown to target at least three proteins in a proteome-wide activity based profiling assay. Among the identified proteins was *a*/*b*-hydrolase domain 6 which is responsible for 2-AG hydrolysis and is implicated in obesity-related metabolic disorders. Due to the similar character of the biarylether and biphenyl moieties, it is possible that the latter may have similar selectivity profiles, but in this current work, selectivity studies are limited to DAGL, MAGL and porcine pancreatic lipase.

The *N*-aryl glycine sulfonamides reported to date possess several potential liabilities. The compounds are very lipophilic as estimated by their *C*Log*P*'s. All contain a carboxylic acid group which would be expected to limit the compounds permeability. In addition, the most potent examples of this chemotype retain an embedded biaryl amine of the type found in compound **3**. Due to the known carcinogenicity of [1,1′-biphenyl]-4-amine,[37,38] we chose to prioritize the identification of suitable replacements for the biphenyl amine group while simultaneously addressing the hydrophobic deficiencies and functional group liabilities.

2. Chemistry

With the objectives outline above, one of the first approaches explored was to insert a spacer between the sulfonamide nitrogen atom and the biaryl ring system. This strategy would obviate the potential for formation of electrophilic phase II metabolites that could result from the oxidation and conjugation of any anilines that might be released from the parent structure.[39] Three general synthetic methods to the targeted compounds (Fig. 4) were used to independently explore the sulfonamide, benzylic amine and biaryl substituents. The first method used an initial sulfonylation of suitably functionalized benzylic amines **A**, followed by alkylation with methyl-2-bromoacetate to provide esters **B**. Hydrolysis of **B** provided intermediate acids **C** that could be subsequently coupled with a range of boronic acids under standard Suzuki–Miyaura[40] conditions to provide the desired compounds **D**, generally in good to excellent yields. The advantage of this synthetic sequence was the ability to control the stereochemistry and substitution at the benzylic position by starting with an appropriately functionalized benzylic amine. The second synthetic method took advantage of commercially available benzyl and biaryl bromides. The *t*-butyl ester of glycine was sulfonylated to give derivatives **E**, which were reacted with the desired benzylic bromides to provide the esters of type **F**. Deprotection with trifluoroacetic acid provided the final compounds **I**. For parallel synthesis it was found that removing the acid protecting group after completing the Suzuki–Miyaura reaction gave more consistent results. Thus, in a third method, *t*-butyl esters **E** were alkylated with either 4- or 3-bromo benzylbromide to provide the intermediates **G**. These intermediates were then coupled with boronic acids to give esters **H** and deprotected to give the targeted compounds **I**.

3. Results and discussion

Table 1 illustrates the observed SAR associated with the introduction of a methylene spacer between the aryl moiety and the nitrogen of the sulfonamide. It was found that the simple benzyl amine derivative **5** showed no DAGL-α inhibition up to the highest concentration tested of 30 μM. However, the combination of a methylene spacer and a *para* phenyl ring, as found in derivative **6**, immediately gave a compound in the 100 nM potency range. Further substitution on the distal phenyl ring produced significant advancements in potency, with several halogenated derivatives exhibiting low double digit nanomolar inhibition. For example, the 2,4-dichloro compound **7** gave a 3-fold improvement over the unsubstituted phenyl compound **6**. Typically, halogens as in compounds **7**–**13**, alkyls and weak hydrogen-bond acceptors as presented in compounds **14**–**16** gave the lowest IC_{50}'s, as illustrated in Table 1. Additionally, the distal aryl group was equally well tolerated in both the *meta*- or *para*-position, as can be seen by comparing analog **7** with **8** and **12** with **13**. In contrast, basic amines and hydrogen bond donors (data not shown) on the terminal phenyl showed significantly poorer activity. The effects of substitution on the methylene spacer were also examined. Introduction of a methyl group produced enantiomers **9** and **10**. Both compounds were approximately 20 nM regardless of the absolute stereochemistry and did not represent a significant improvement over compound **7**. Di-substitution in the form of a cyclopropyl or a cyclobutyl group showed interesting SAR. A significant loss in potency was observed with cyclopropyl relative to the unsubstituted or mono-methyl substituted analogs, as can be

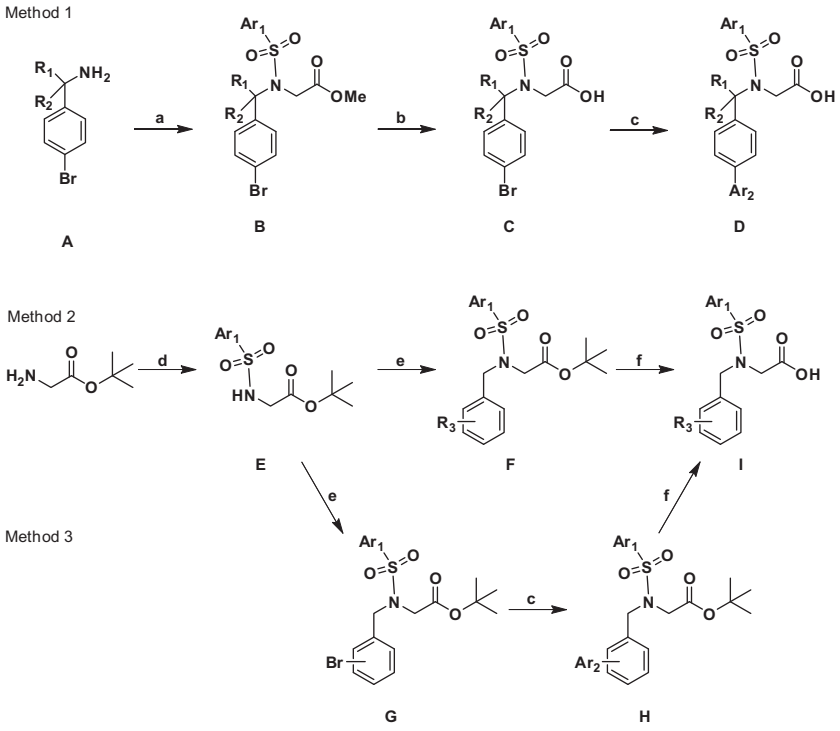

Figure 4. (a) (i) Aryl sulfonyl chloride, DIEA, DMF, 70 °C; (ii) methyl-2-bromoacetate, BEMP, 80 °C. (b) NaOH, MeOH, THF. (c) Arylboronic acid, sodium bicarbonate (aq), palladium acetate, DMF, 120 °C. (d) Aryl sulfonyl chloride, pyridine, DMAP, DCM. (e) Benzyl bromide, BEMP, 70 °C. (f) TFA.

observed with the cyclopropyl compound **11** having an IC_{50} of 130 nM. A similar loss of potency was observed with cyclopropyl derivative **15** versus the unsubstituted analog **14** with IC_{50}s of 40 and 17 nM, respectively. However, increased ring size resulted in an improvement as observed with cyclobutyls such as **12**, **13** and **16** that have IC_{50}s of 7, 11 and 8 nM, respectively. A possible explanation for the reduced activity observed with the cyclopropyl analogs could be attributed to the larger bond angle (~115°) between geminal pendant substituents on the smaller cyclopropyl ring relative to the larger cyclobutyl (~112°) or acyclic derivatives (~109°). While these differences are modest, the associated quaternary carbon is at the center of the molecule, and even small changes in bond angles here could result in significant differences in the relative positions of distal portions of the analogs examined. As discussed above, and as will be presented below, the terminal moieties in the compounds are key determinants of the potencies observed. However, the similar activities observed for the *para*- and *meta*-biaryls seen in **12** and **13** suggests that small changes in the placement of the distal substituents should be tolerated. An alternative explanation for the observed SAR is that di-substitution at the benzylic position is suboptimal, but can be overcome by increasing lipophilicity in the form of larger saturated rings. A full understanding of these observations will have to await a co-crystal structure. However, from the data presented it is apparent that the cyclobutyl derivative **13** represented an excellent compromise. This compound significantly increased potency with a minimum addition of lipophilicity, and was therefore chosen as a starting point for further optimization.

With the initially identified preferred substituents at both the benzylic position and the terminal aryl of the biphenyl group, we turned our attention to the optimization of the sulfonamide moiety. Table 2 shows the SAR for substitution of the sulfonamide aryl ring while holding the cyclobutyl spacer and the biphenyl substituents constant.

As a reference point, 2-(*N*-(1-(3′,5′-dichloro-[1,1′-biphenyl]-3-yl)cyclobutyl) phenyl-sulfonamido)acetic acid (**17**) was determined to have an IC_{50} of 80 nM. It was found that in all cases examined, *ortho* substitution negatively impacted activity, as typified with analogs **18** and **23**. Contrastingly, *meta* substitution had either modest or no effect, as characterized by compounds **19** and **22**. More encouraging was the observation that *para* substitution significantly improved activity, as observed with analogs **20**, **21**, **13** and **24**. In general, it would appear that electron rich sulfonamides are more active, as the potency order follows the sequence of increasing electron donating character of the substituents, that is, 2,2-dimethylchromanyl > F_2HCO- > -Cl > -CN. Consistent with this observation were the results obtained in attempting to introduce isosteric heterocycles at this vector (data not shown). A variety of such heterocycles showed a significant loss in potency and were not considered viable replacements for phenyl. It is interesting however, that heteroatoms are tolerated when masked with adjacent lipophilicity, as in 2,2-dimethylchromanyl derivative **24** that displayed sub-nanomolar (0.6 nM) potency. Given this finding, 2,2-dimethylchromanyl derivatives were used to reexamine the SAR at the benzylic position of the chemotype.

Benzylic derivatives were prepared and typical trends can be seen in Figure 5. The unsubstituted compounds **25** and **26** showed a four-fold loss in potency relative to the cyclobutyl derivative, **24**. It was also observed that the cyclobutyl **24** and cyclopentyl **27** groups were approximately equipotent with IC_{50}s of 0.6 and 0.9 nM, respectively. In an attempt to investigate the tolerance for polarity in this region of the structure, the tetrahydrofuran derivative **28** was prepared and a ten-fold loss in activity (IC_{50} 8 nM) versus the cyclopentyl compound **27** was observed. At this juncture, it was concluded that the preferred pendent moieties consisted of cyclobutyl, 2,2-dimethylchromanyl sulfonyl and either a *meta* or *para* 3,5-dichlorophenyl group. With these significant advancements, our focus shifted to optimization of the glycine core.

Efforts to replace the carboxylic acid moiety with esters, amides or a variety of common acid isosteres were uniformly unsuccessful resulting in almost complete loss of activity (data not shown). It

Table 1
IC_{50}'s for DAGL-α inhibition were determined in a cell-free assay at pH 6.5 as previously described[41]

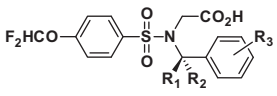

	R_1/R_2	R_3 position	R_3	DAGL-α IC_{50} (nM)
5	H/H	*para*	H	>30,000
6	H/H	*para*	Ph	80 ± 50 (n = 2)
7	H/H	*meta*	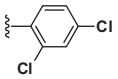	30 ± 15 (n = 2)
8	H/H	*para*	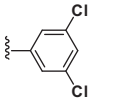	16 ± 10 (n = 2)
9	H/CH_3	*para*	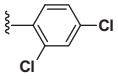	18 ± 5 (n = 3)
10	CH_3/H	*para*	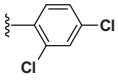	19 ± 6 (n = 3)
11	Cyclopropyl	*para*	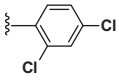	130 ± 65 (n = 4)
12	Cyclobutyl	*para*	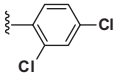	7 ± 4 (n = 5)
13	Cyclobutyl	*meta*	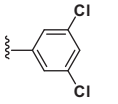	11 ± 7 (n = 3)
14	H/H	*para*	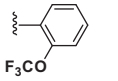	17 ± 6 (n = 5)
15	Cyclopropyl	*para*	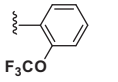	40 ± 10 (n = 3)
16	Cyclobutyl	*para*	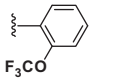	8 ± 3 (n = 3)

was also found that substitution is not tolerated alpha to the carboxylic acid, nor is homologation of the acid. For example, alanine or β-alanine derivatives displayed no inhibitory activity. Finally, the sulfonamide linkage was found to be required. Benzyl carbamate, phenyl urea and benzamide derivatives were inactive at the highest tested concentrations. Taken collectively, these requirements suggest a very specific, sterically constrained interaction between the inhibitor's carboxylic acid head group and the enzyme. In contrast, the SAR of the *N*-alkyl and *N*-sulfonyl groups tolerates a wide variety of lipophilic functionality consistent with these groups binding in a flexible or large lipophilic pocket. Recalling that DAGL is a serine hydrolase and that lipophilic DAG is its substrate, it is tempting to suggest that the inhibitors operate through a four point pharmacophore model (Fig. 6). In this model, the carboxylic acid could form a hydrogen bond or a salt bridge interaction near the active site: perhaps interacting with one of the catalytic residues of the proton transfer network. The tetrahedral sulfonyl moiety could act as a transition-state mimetic, accept critical hydrogen bonds from complimentary donors near the active site, or act to control the conformation. Finally, the large lipophilic groups can occupy pockets normally occupied by the hydrocarbon chains of the endocannabinoid substrate esters. Alternatively, it is also possible that the two lipophilic side chains undergo hydrophobic collapse and fill a larger, common binding site. Currently, no X-ray crystal structures of human DAGLs are reported that would help further refine this putative pharmacophore.

However, a homology model for the active site of DAGL-α has been proposed. The model is based on the co-crystal structure of oleic acid bound to *Thermomyces (Humicola) lanuginosa* S146A mutant.[42] This serine hydrolase and DAGL-α contain the same Ser-His-Asp catalytic triad and typical α/β hydrolase fold motif.[43] The docking of compound **4** into the model has been described to provide two complimentary, high-ranking binding poses.[36] In one pose, the carboxylic acid forms a hydrogen bond with the catalytic serine (Ser472). In the second pose the carboxylic acid forms a hydrogen bond with the catalytic histidine (His650) and a second nearby histidine (His471). In both poses the aryl rings occupy separate, large, open hydrophobic pockets. The sulfonamide forms no direct interactions with DAGL-α in this model, but instead acts as a geometrical constraint to place the aryl rings into the hydrophobic pockets. By extension, it would be concluded that the substituents on the benzylic methylene of our inhibitors would point into the solvent in both poses. Thus the reported homology model does not readily explain the SAR observed when comparing compounds **27** (0.9 nM) and **28** (8 nM). Nonetheless, even without a conclusive binding hypothesis, the key elements required for highly-potent, non-covalent inhibitors of DAGL-α have been successfully defined, and our attention progressed to an assessment of the physiochemical characteristics of this series of compounds.

From the structures above, it can be clearly seen that the best inhibitors are highly lipophilic. The requirement for lipophilicity

Table 2
IC_{50}'s for DAGL-α inhibition were determined in a cell-free assay at pH 6.5 as described above for Table 1

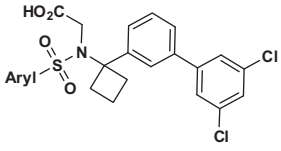

	Aryl	DAGL-α IC_{50} (nM)
17		80 ± 50 (n = 4)
18		510 ± 120 (n = 4)
19	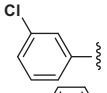	60 ± 30 (n = 4)
20	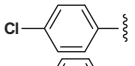	4 ± 1 (n = 4)
21	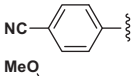	45 ± 10 (n = 4)
22	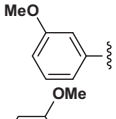	161 ± 40 (n = 4)
23		14,000 ± 3,100 (n = 4)
13	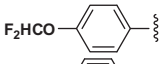	11 ± 7 (n = 3)
24	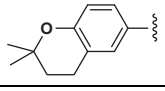	0.6 ± 0.1 (n = 5)

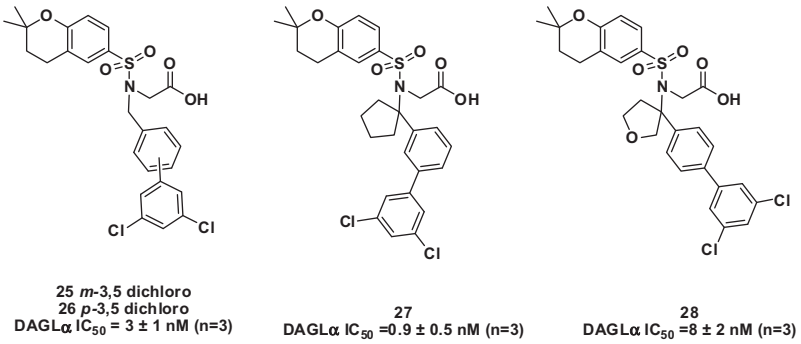

Figure 5. Key analogs used to characterize SAR at the benzylic position.

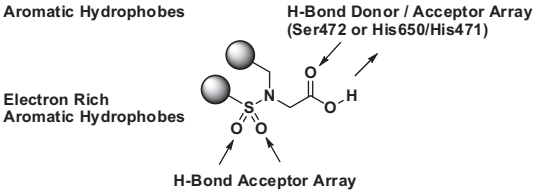

Figure 6. Rudimentary 4-point pharmacophore model consistent with observed SAR. Conserved amino acid residues in parenthesis have the potential to form interactions based on the reported homology model.

is not surprising considering the nature of the DAGL substrate (DAG; *C*Log*P* = 6.9), and suggests that the active site of the enzyme has a complimentary highly hydrophobic character. In addition, many lipases access their substrates by maintaining an intimate contact with the cell membrane, where the substrates are located.[43] Inhibitors with high LogPs would be expected to partition into the cell membrane, thereby increasing access to the enzyme's active site.

To fully characterize the lipophilicity of the inhibitors described we compared their *C*Log*P* values with the corresponding measured Log*D*s at a pH of 7.4. Interestingly, the experimentally determined values were consistently and very significantly lower than the *C*Log*P*s for all the analogs profiled. As can be seen in Table 3, the measured Log*D*s were approximately 4 log units less than the calculated LogPs. This discrepancy could be explained primarily through the measured pK_as. Of the analogs characterized, all have pK_as of <3.5. This is appreciably lower than might be expected for a typical carboxylic acid (~4.8), but is consistent with what is expected from an amino acid. Additionally, the lower Log*D*s may also indicate that the compounds undergo a hydrophobic collapse in aqueous solution, minimizing the exposed hydrophobic surfaces and thus reducing their overall hydrophobicity.

Given the highly acidic nature of this inhibitor class, the permeability of this series was of obvious interest and was determined in a parallel artificial membrane permeability assay (PAMPA)[44] at pHs of 5.5 and 7.4 (to simulate pH conditions in the small intestine and blood, respectively). All of the compounds were found to be highly permeable at the lower pH, and not surprisingly, showed a significant reduction in permeability at pH 7.4. Importantly however, the more active examples of the chemotype, as exemplified by compound **29**, maintained high permeability at both pHs examined.

With the permeability of the series characterized, we next explored the activity of the inhibitors in a whole-cell system. In the assay used, DAGL-α was transiently expressed in HEK cells, and 2-AG concentrations were determined directly by mass spectrometry.[41] The results obtained with a representative set of analogs are shown in Table 4.

In the case of the 4-(difluoromethoxy)benzenesulfonyl derivatives, **32**, **16**, **33** and **10**, there is good concordance between the cell-based assay and the enzyme assay, with a consistently modest 5-fold difference in the IC_{50}'s observed between the two assay formats. However, for the 2,2-dimethylchroman-6-sulfonyl derivatives **24** and **12**, there is a larger and more significant decrease in activity in the whole cell assay, with IC_{50}'s that are right shifted, 74 and 15-fold respectively. In the case of **24**, this compound appears quite permeable in our PAMPA assay suggesting that it should readily penetrate into cell membranes to access DAGL. Thus, there is no correlation observed between PAMPA permeability and fold shift in potency in the whole-cell assay system. The shift in activity is not readily explained other than by invoking some non-defined binding to a component of the medium for the cell-based assay.

Regardless, the most important observation from Table 4 is that all of the compounds presented display considerable inhibitory activity against DAGL-α under the more physiologically relevant conditions of a cell-based assay. Of greatest import, is the observation that the reported compounds exhibit activities in both the enzyme and cell-based assays that are similar to those observed for the irreversible inhibitors. Tetrahydrolipstatin (**1**), for example, has an IC_{50} of 1 nM in the enzyme assay and 20 nM in the cell-based assay. Thus, the glycine sulfonamide chemotype clearly demonstrates that a chemically reactive inhibitor is not required for potent activity against DAGL in a cellular context. Hence, it has been established that this enzyme can be targeted by conventional means, opening the door to future drug design.

As detailed in the introduction, a key objective in the identification of chemically non-reactive inhibitors of DAGL was the hope that they would display significant selectivity against other serine hydrolases to avoid potential off-target effects. To that end we first explored the selectivity of a number of our analogs against DAGL-β, with representative data being presented in Table 5. Interestingly, all of the compounds displayed selectivity for DAGL-α over DAGL-β, with factors ranging between 5 and 70-fold within the structural diversity explored. However, it should be noted that the most potent compounds do retain significant inhibitory activity against DAGL-β, and any observed in vivo effects could potentially be attributed to inhibition of either or a combination of both isoforms.

Additionally, all of the compounds presented above showed no activity in assays that measure their inhibitory profile against either MAGL or porcine pancreatic lipase (PPL) at test concentrations up to 30 μM. Thus the compounds are not expected to be indiscriminant lipase inhibitors, although a more comprehensive profiling in this regard is certainly merited.[36]

To assess if our compounds could be useful as tools for in vivo proof of concept studies, and to gain further perspective on their drug-like properties, we conducted some additional profiling studies, the results of which are shown in Table 6.

Table 3
Physico-chemical and permeability analyses of select examples of DAGL inhibitors

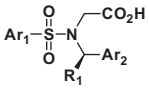

	Ar_1	Ar_2	R_1	DAGL-α IC_{50} (nM)	CLogP	Log*D* pH 7.4	PAMPA pH 5.5	PAMPA pH 7.5	pK_a
29	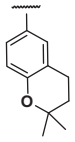	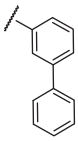	H	55 ± 60 (*n* = 4)	6.6	2.2	630	430	3.4
5	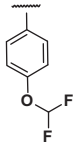		H	>30,000	3.6	−0.4	290	<15	3.4
30	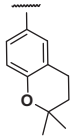	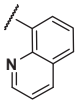	H	13,500 ± 6000 (*n* = 4)	4.6	0.5	550	75	2.0/5.8
31	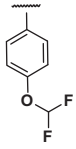		CH_3	16,000 (*n* = 1)	3.9	−0.3	537	32	3.4

The analogs profiled span approximately two orders of magnitude with respect to their potency of inhibition of DAGL-α. With respect to their potential for metabolic clearance, as assessed in a liver microsome assay,[45] all show potential for moderate clearance in the rodent species examined, and somewhat lower potential for clearance in humans. All of the compounds displayed some minor activity in a flux assay[46] used to determine blocking of the human ether-a-go-go (HERG) channel, and would require further characterization in an electrophysiology patch clamp assay to more accurately determine the significance of this observation. We also assessed the analogs ability to inhibit a panel of cytochrome P450 (CYP) enzymes,[47] with selected data reported above. While none of the analogs displayed particularly potent inhibition of any of the isozymes, the data suggest that the free methylene derivatives **29** and **33**, display better CYP profiles than their di-substituted congeners **24** and **16**. Additionally, we noted that compound **24** displayed significant activity in a pregnane transactivation (PXR) assay,[48] and further profiling of this compound and related analogs could be warranted to fully assess the potential for auto-induction of metabolism. However, in a general sense as it relates to the chemotype, all of the signals observed in the profiling assays described above appear sporadic in nature. We concluded that the chemotype did not possess any implicit liabilities in the profiling suite described above and therefore provides an excellent lead for continued drug-design efforts.

Given the outstanding potency of compound **24** in both the enzyme and whole-cell assays, its pharmacokinetic (PK) profile was examined in mice. The results from these experiments are shown in Table 7.

In all three dosing formats the maximal exposure (C_{max}) of **24** far exceeds its measured whole-cell IC_{50} of 40 nM. From the IV study the observed large volume of distribution (7.4 L/Kg) is consistent with good distribution into the tissues, which is interesting given the highly acidic nature of the compound. The compound also displayed a very high rate of clearance (Cl), which may reflect sustained partitioning into membranes. However, **24** did have excellent bioavailability when administered either IP or PO with F values of 100% and 88%, respectively. The high bioavailability suggests that first pass metabolism via the liver is minimal; a result consistent with the modest in vitro clearance in liver microsomes. The high clearance observed in the IV study (twice hepatic blood flow) is also consistent with non-hepatic mechanisms. In separate studies (data not disclosed) the brain uptake of **24** was explored, and no significant penetration into the CNS was observed. This is consistent with other members of this series that were also examined in brain uptake studies and were shown not to penetrate into the brain. Thus it is expected that these compounds would achieve sufficient concentrations to act exclusively on peripherally located DAGLs.

4. Conclusion

We have described the structure activity relationships, profiling characteristics and physico-chemical properties for the first reported series of *N*-benzylic-substituted glycine sulfonamides that reversibly inhibit diacylglycerol lipases. An effort to identify replacements for a known toxicophore led to the identification of 2-(*N*-(1-(3′,5′-dichloro-[1,1′-biphenyl]-3-yl)cyclobutyl)-2,2-dimethylchroman-6-sulfonamido)acetic acid **24**. This compound is a highly potent, easily-prepared inhibitor of DAGL alpha and beta that lacks the embedded biphenyl amine found in our initially identified leads. In contrast to nearly all previously reported DAGL inhibitors, this compound is not an irreversible inhibitor of the DAGLs. The compound has sub-nanomolar activity versus the alpha isoform and nanomolar activity versus the beta isoform. A window of roughly 60-fold exists between the activities versus the two isoforms and there is no activity versus other lipases tested. The compound also has excellent activity in a whole-cell

Table 4
Comparison of enzyme and whole-cell inhibitory assay data

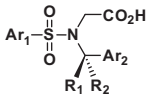

	Ar_1	Ar_2	R_1/R_2	DAGL-α IC_{50} (nM)	Whole cell IC_{50} (nM)	PAMPA pH 5.5	Fold loss in activity
24	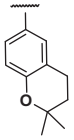	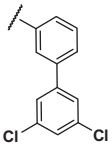	Cyclobutyl	0.6 ± 0.1 (n = 5)	37 (n = 1)	288	74
32	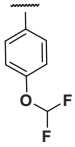	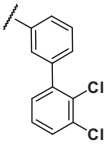	H/H	3 ± 2 (n = 9)	14 ± 9 (n = 5)	ND	5
12	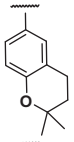	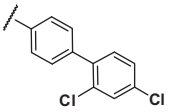	Cyclobutyl	6 ± 4 (n = 5)	88 ± 25 (n = 2)	ND	15
16	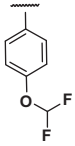	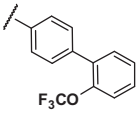	Cyclobutyl	22 ± 7 (n = 4)	82 ± 30 (n = 2)	179	4
33	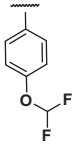	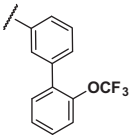	H/H	17 ± 8 (n = 7)	60 ± 10 (n = 2)	455	4
10	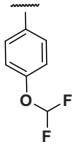	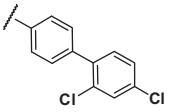	CH_3/H	19 ± 6 (n = 3)	100 ± 70 (n = 2)	500	5

assay, and a promising pharmacokinetic profile. The compound was found to have no access to the CNS and would be expected to avoid the CNS side-effects observed with CB_1 antagonist rimonabant and the inverse agonist taranabant while having therapeutic potential for diet-induced obesity and metabolic syndrome. We anticipate **24** to be a valuable tool compound for studying DAGL inhibition, and constitute an important lead for future medicinal chemistry efforts.

5. Experimental section

5.1. General considerations

All reagents were purchased from commercial suppliers and used without purification. All anhydrous reactions were performed under a nitrogen or argon atmosphere using SureSeal™ solvents from Aldrich. Proton nuclear magnetic resonance (^{1}H NMR) spectra were recorded on a Varian 600 MHz spectrometer, on a Bruker Avance III 400 MHz or 500 MHz spectrometer, each equipped with a 5-mm TXI or BBFO probe. All spectra were determined in the solvents indicated and chemical shifts are reported in parts per million (ppm) δ units downfield from the internal standard tetramethylsilane (TMS) with inter proton coupling constants reported in Hertz (Hz). Multiplicity patterns are designated as follows: s, singlet; d, doublet; t, triplet; q, quartet; m, multiplet; br, broad; dd, doublet of doublet; dt, doublet of triplet; dq, doublet of quartet and most spectra were analyzed using the ACDLABS SpecManager™ 12.0 program software. Reactions performed under microwave irradiation utilized either a Biotage Initiator or CEM Discover microwave. Liquid chromatography (LC)–mass spectra (MS) were run on a Shimadzu LC instrument coupled to a Waters Micromass ZQ instrument. All final compounds had purity $\geqslant$95%, unless otherwise noted. LC–MS and HPLC conditions are provided in the Supplementary material.

5.1.1. 2-(*N*-Benzyl-4-(difluoromethoxy)phenylsulfonamido) acetic acid (5)

To a solution of *tert*-butyl 2-aminoacetate hydrochloride (0.864 g, 5.00 mmol) in dichloromethane (10 mL) was added pyridine (4.04 mL, 50.0 mmol), 4-(difluoromethoxy)benzene-1-sulfonyl chloride (1.213 g, 5 mmol) and a catalytic amount of dimethylaminopyridine. The reaction mixture was stirred at room temperature overnight. The crude reaction mixture was diluted with ethyl acetate and the organic layer was washed once each with brine and sodium bicarbonate. The organic portion was dried over sodium sulfate. The solvent was removed in vacuo and the

Table 5
DAGL selectivity profiling for prototypical inhibitors

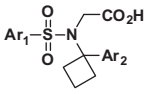

	Ar_1	Ar_2	DAGL-α IC_{50} (nM)	DAGL-β IC_{50} (nM)	Fold difference
24	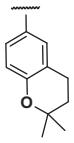	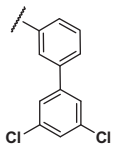	0.6 ± 0.1 (n = 8)	40 ± 16 (n = 2)	67
34	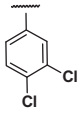	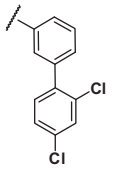	6 ± 3 (n = 3)	80 (n = 1)	13
12	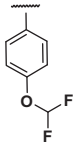	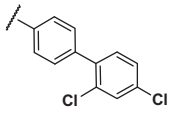	6 ± 4 (n = 5)	146 (n = 1)	24
16	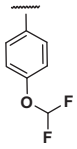	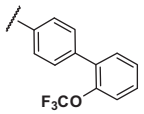	22 ± 7 (n = 4)	112 (n = 1)	5

residue was purified with a gradient of 10:1 hexane/ethyl acetate to 3:2 hexane/ethyl acetate on a 40 g silica gel column. The fractions containing the product were collected and concentrated to afford *tert*-butyl ((4-(difluoromethoxy)phenyl)sulfonyl)glycinate as white solid (0.95 g, 54%). ^{1}H NMR (500 MHz, chloroform-*d*) δ ppm 7.87 (d, J = 9.0 Hz, 2H), 7.22 (d, J = 9.0 Hz, 2H), 6.58 (t, J = 75 Hz (C-F), 1H), 5.09 (t, J = 5.5 Hz (N–H), 1H), 3.68 (d, J = 5.5 Hz, 2H), 1.34 (s, 9H). LC–MS 1.2 min, 336.0 (M−H).

Benzyl bromide (10.64 μL, 0.089 mmol) was added to an acetonitrile (1.0 mL) solution of *tert*-butyl ((4-(difluoromethoxy) phenyl)sulfonyl)glycinate (20 mg, 0.059 mmol) followed by 2-*tert*-butylimino-2-diethylamino-1,3-dimethylperhydro-1,3,2-diazaphosphorine (BEMP) on resin (53.2 mg, 0.107 mmol). The mixture was agitated at 70 °C overnight. The solvent was removed and dichloromethane (2.0 mL) was added. The mixture was filtered to remove the resin. TFA (0.7 mL) was added. After 1 h an LC–MS showed the reaction was complete. The solvent was removed and the crude material dissolved in methanol and purified using preparative HPLC employing acetonitrile/water and 0.1% TFA buffer with a 30 mm × 100 mm Xterra™ column. The fractions containing the desired product were combined. The solvent was removed in vacuo and the title compound obtained as a white solid (20 mg, 86%). ^{1}H NMR (500 MHz, chloroform-*d*) δ ppm 3.96 (s, 2H), 4.47(s, 2H), 6.58 (t, J = 75 Hz (C-F), 1H), 7.20–7.26 (m, 4H), 7.32 (m, 3H), 7.89 (d, J = 11.5, 2H). LC–MS 0.78 min, 372.2 (M+H), 370.2 (M−H).

5.1.2. Compounds 6, 7 and 8

Compounds **6**, **7** and **8** were prepared as part of a larger parallel synthesis library from *t*-butyl *N*-(4-bromobenzyl)-*N*-((4-(difluoromethoxy)phenyl) sulfonyl) glycinate.

5.1.2.1. *t*-Butyl *N*-(4-bromobenzyl)-*N*-((4-(difluoromethoxy) phenyl) sulfonyl) glycinate. This common intermediate was prepared from 1-bromo-4-(bromomethyl)benzene and *tert*-butyl ((4-(difluoromethoxy)phenyl)sulfonyl)glycinate using the method described in the preparation of **5**. ^{1}H NMR (500 MHz, methanol-d_4) δ ppm 7.96–7.90 (m, 2H), 7.53–7.46 (m, 2H), 7.34 (d, J = 8.9 Hz, 2H), 7.22 (d, J = 8.2 Hz, 2H), 7.19–6.86 (m, 1H), 4.47 (s, 2H), 3.86 (s, 2H), 1.35 (s, 9H).). LC–MS: 2.3 min, no ion observed.

5.1.2.2. Parallel synthesis method. *t*-butyl *N*-(4-bromobenzyl)-*N*-((4-(difluoromethoxy)phenyl) sulfonyl) glycinate. (1.2 g) was dissolved in 23.5 mL of anhydrous NMP. Microwave vials containing the appropriate boronic acid (0.062 mmol, 1.2 equiv) were prepared. The bromide solution (0.5 mL) was added to each microwave vial. Potassium carbonate (77.0 μL, 2 N, 3 equiv, 0.154 mmol), 3.8 mg of $PdCl_2$(dppf) (5.13 μmol, 0.1 equiv) were added to each vial followed by 0.1 mL of anhydrous NMP to wash the solids off the sides of the vial. The vials were capped, flushed with a blanket of Argon and heated in a microwave reactor at 150 °C for 30 min, pre-stirring was 10 s. Five samples were randomly chosen and all contained desired product by LC/MS analysis. The samples were dried overnight under vacuum centrifugation. The residue in each microwave vial (expected 1 equiv, 0.051 mmol) was dissolved in 0.5 mL of anhydrous dichloromethane. To each of the vials was added 0.5 mL of TFA and the solution stirred for 4 h. LC–MS of randomly chosen samples showed complete reaction. The samples were dried overnight under vacuum centrifugation. To each microwave vial was added 0.6 mL DMSO and 1.0 mL of dimethylformamide. The vials were sonicated and shaken for 10 min. The solids were removed by filtration and purified on a 19 × 100 mm 5 μm Waters Xbridge™ C18 column with acetonitrile and aqueous ammonium acetate.

5.1.2.3. 2-(*N*-([1,1′-Biphenyl]-4-ylmethyl)-4-(difluoromethoxy) phenylsulfonamido) acetic acid (6). ^{1}H NMR (600 MHz, dimethyl sulfoxide-d_6 chloroform-*d*) δ ppm 7.92 (d, J = 8.2 Hz, 2H), 7.61 (d, J = 7.6 Hz, 2H), 7.58 (d, J = 7.6 Hz, 2H), 7.46 (t, J = 63 Hz (CHF_2), 1H), 7.44 (t, J = 7.3 Hz, 2H), 7.36–7.28 (m, 5H), 4.47 (br s, 2H), 3.87 (br s, 2H). LC–MS: 3.5 min, 446.5 (M−H).

5.1.2.4. 2-(*N*-((2′,4′-Dichloro-[1,1′-biphenyl]-4-yl)methyl)-4-(difluoromethoxy) phenylsulfonamido) acetic acid (7). ^{1}H NMR (600 MHz, dimethyl sulfoxide-d_6 chloroform-*d*) δ ppm 7.91 (d, J = 7.6 Hz, 2H), 7.63 (br s, 1H), 7.45 (d, J = 8.8 Hz, 1H),

Table 6
General profiling of selected benzylic analogs

Compound	Metabolic stability % remaining			HERG IC_{50} (μM)	Cyp IC_{50} (μM)				PXR EC_{50} (μM)/% activation
	Human	Rat	Mouse		2C19	2C9	2D6	3A4	
24	79	70	77	40	9	3	13	9	3/140
16	78	100	100	15	13	27	4	6	ND
33	80	100	ND	11	40	40	40	30	ND
29	77	67	87	20	40	23	40	40	ND

Details of the assays can be found in the Supplementary material.

Table 7
Pharmacokinetic profile of **24** in mice ($N = 4$) when dosed intravenously (IV), orally (PO), or intraperitoneally (IP)

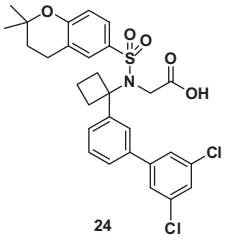

24

Route/dose (mg/kg)	$t_{1/2}$ (h)	C_{max} (nM)	T_{max} (h)	AUCinf (nM*h)	Cl (mL/min/kg)	Vss (L/kg)	F (%)
IV/1	0.58 ± .05	274 ± 40	–	173 ± 14	168.7 ± 13.6	7.42 ± 0.94	–
PO/10	0.99 ± .08	941 ± 68	0.5 ± 0.1	1516 ± 123	–	–	88 ± 7
IP/10	1.33 ± .25	2863 ± 410	0.63 ± 0.25	5784 ± 640	–	–	~100

7.40–7.35 (m, 3H), 7.34–7.30 (m, 4H), 7.18 (s, (CHF_2), 1H), 4.50 (s, 2H), 3.90 (s, 2H). LC–MS 4.1 min, 513.8 (M−H).

5.1.2.5. 2-(*N*-((3′,5′-Dichloro-[1,1′-biphenyl]-3-yl)methyl)-4-(difluoromethoxy) phenylsulfonamido) acetic acid (8).

^{1}H NMR (600 MHz, dimethyl sulfoxide-d_6 chloroform-d) δ ppm 7.91 (d, J = 8.2 Hz, 2H), 7.61–7.58 (m, 3H), 7.52 (br s, 1H), 7.42 (d, J = 8.2 Hz, 1H), 7.33–7.27 (m, 4H), 7.18 (s, (CHF_2), 1H), 4.49 (s, 2H), 3.91 (s, 2H). LC–MS 4.4 min, 514.5 (M−H).

5.1.3. (*S*)-2-(*N*-(1-(2′,4′-dichloro-[1,1′-biphenyl]-4-yl)ethyl)-4-(difluoromethoxy) phenylsulfonamido) acetic acid (9)

To a solution of (*S*)-(−)-1-(4-Bromophenyl)ethylamine (0.078 mL, 0.500 mmol) and *N,N*-diisopropylethylamine (0.131 mL, 0.750 mmol) in dimethylformamide (1.0 mL), 4-(difluoromethoxy)benzene-1-sulfonyl chloride (121 mg, 0.500 mmol) was added. The reaction mixture was stirred at room temperature for 1 hour. LC–MS analysis showed the reaction was complete: 1.4 min, 404.1, 406.1 (M−H) Methyl bromoacetate (0.095 mL, 1.000 mmol) and BEMP (274 mg, 1.000 mmol) were added to the reaction containing crude (*S*)-*N*-(1-(4-bromophenyl)ethyl)-4-(difluoromethoxy)benzenesulfonamide and the reaction was heated at 70 °C overnight. The reaction was diluted with ethyl acetate and washed with water and brine. The organic portion was dried over sodium sulfate. The solvent was removed, the residue dissolved in methanol and purified by preparative HPLC using a CH_3CN–H_2O-TFA solvent system. Obtained methyl (*S*)-*N*-(1-(4-bromophenyl)ethyl)-*N*-((4-(difluoromethoxy)phenyl) sulfonyl) glycinate as light yellow oil.

^{1}H NMR (500 MHz, chloroform-d) δ ppm 1.49 (d, J = 6.71 Hz, 3H) 3.79 (d, J = 18.31 Hz, 1H) 4.06 (d, J = 18.62 Hz, 1H) 5.15 (q, J = 6.82 Hz, 1H) 6.61 (t, J = 75.00 Hz, 1H) 7.20–7.27 (m, 5H) 7.27–7.35 (m, 3H) 7.48 (s, 1H) 7.97 (d, J = 8.55 Hz, 2H). LC–MS 1.3 min 531 (M+H).

To a toluene (1.5 mL) and ethanol (1.5 mL) solution of methyl (*S*)-*N*-(1-(4-bromophenyl)ethyl)-*N*-((4-(difluoromethoxy)phenyl) sulfonyl) glycinate (60 mg, 0.125 mmol) was added 2,4-dichlorophenylboronic acid (28.7 mg, 0.151 mmol), followed by Na_2CO_3 (1 N, 0.8 mL) and tetrakis(triphenylphosphine)palladium (0) (7.25 mg, 6.27 μmol). The mixture was degassed, placed under argon and heated at 120 °C in microwave reactor for 30 min. LC–MS analysis showed that the reaction was complete. The mixture was diluted with ethyl acetate and extracted with brine. The organic portion was dried over sodium sulfate. The solvent was removed and residue purified using preparative HPLC employing acetonitrile and water containing 0.1% TFA on an Xterra™ 30 mm × 100 mm column. The solvent was removed from the fractions containing the desired product. A colorless oil (12 mg, 17% yield) was obtained. ^{1}H NMR (500 MHz, chloroform-d) δ ppm 7.97 (d, J = 8.5 Hz, 2H), 7.48 (s, 1H), 7.32 (d, J = 8.2 Hz, 2H), 7.29 (d, J = 8.2 Hz, 1H), 7.25 (d, J = 4.3 Hz, 3H), 7.24–7.20 (m, 2H), 6.82–6.39 (m, 1H), 5.15 (q, J = 6.8 Hz, 1H), 4.06 (d, J = 18.6 Hz, 1H), 3.79 (d, J = 18.3 Hz, 1H), 1.56–1.43 (m, 3H). LC–MS 1.1 min, 528.2 (M−H). HRMS Calcd for $C_{23}H_{18}O_5NCl_2F_2S$: 528.0245. Found: 528.0247.

5.1.4. (*R*)-2-(*N*-(1-(2′,4′-Dichloro-[1,1′-biphenyl]-4-yl)ethyl)-4-(difluoromethoxy) phenylsulfonamido) acetic acid (10)

Prepared from (*R*)-(−)-1-(4-Bromophenyl)ethylamine in the same manner as compound **9**. ^{1}H NMR (500 MHz, chloroform-d) δ ppm 1.50 (d, J = 7.02 Hz, 3H) 3.79 (d, J = 18.31 Hz, 1H) 4.07 (d, J = 18.31 Hz, 1H) 5.15 (q, J = 7.02 Hz, 1H) 6.61 (t, J = 75.00 Hz, 1H) 7.20–7.25 (m, 5H) 7.29 (d, J = 8.24 Hz, 1H) 7.32 (d, J = 8.24 Hz, 2H) 7.48 (s, 1H) 7.97 (d, J = 8.55 Hz, 2H). LC–MS 1.1 min, 528.2 (M−H), Exact Mass: 529.0. HRMS Calcd for $C_{23}H_{18}O_5NCl_2F_2NaS$: 552.0221. Found: 552.0208.

5.1.5. 2-(*N*-(1-(3′,5′-Dichlorobiphenyl-3-yl)cyclopropyl)-4-(difluoromethoxy) phenylsulfonamido) acetic acid (11)

Prepared from 1-(4-bromophenyl)cyclopropanamine in the same manner as compound **9**.

^{1}H NMR (500 MHz, chloroform-d) δ ppm 1.29 (br s, 2H) 1.68 (br s, 2H) 4.36 (s, 2H) 6.56 (t, J = 75.00 Hz, 1H) 7.10 (m, J = 8.85 Hz, 2H) 7.19–7.24 (m, 3H) 7.24–7.31 (m, 1H) 7.31–7.36 (m, 2H) 7.52 (d, J = 1.83 Hz, 1H) 7.76 (m, J = 8.85 Hz, 2H). LC–MS 1.1 min, 539.9 (M−H). HRMS Calcd for $C_{24}H_{18}O_5NCl_2F_2S$: 540.0245. Found: 540.0246.

5.1.6. 2-(*N*-(1-(2′,4′-Dichlorobiphenyl-4-yl)cyclobutyl)-4-(difluoromethoxy) phenylsulfonamido) acetic acid (12)

4-(Difluoromethoxy)benzene-1-sulfonyl chloride (170 mg, 0.700 mmol) was added to a solution of 1-(4-bromophenyl)cyclobutanamine HCl (184 mg, 0.7 mmol) and BEMP (384 mg, 1.400 mmol) in dimethylformamide (1.0 mL). The reaction mixture was stirred at 70 °C overnight. Methyl bromoacetate (0.133 mL, 1.400 mmol) and additional BEMP (384 mg, 1.400 mmol) was added and the reaction heated at 70 °C overnight. The reaction was diluted with ethyl acetate and washed with HCl (1 N) and brine. The organic portion was dried over sodium sulfate.The residue was purified by chromatography using 4:1 hexanes/ethyl acetate on a 40 g silica column to give methyl 2-(*N*-(1-(4-bromophenyl)cyclobutyl)-4-(difluoromethoxy)phenylsulfonamido) acetate as a yellow oil (200 mg, 57% yield).

^{1}H NMR (500 MHz, $CDCl_3$) δ ppm 1.69 (d, J = 10.68 Hz, 1H), 1.83–1.92 (m, 1H), 2.67 (t, J = 8.70 Hz, 2H), 2.79–2.91 (m, 2H), 4.13 (s, 2H), 6.54 (t, J = 75.00 Hz, 1H), 7.06 (d, J = 8.55 Hz, 2H), 7.22–7.31 (m, 1H), 7.37 (d, J = 8.24 Hz, 3H), 7.47–7.58 (m, 5H). LC/MS 1.5 min, Molecular ion not observed.

Methyl 2-(*N*-(1-(4-bromophenyl)cyclobutyl)-4-(difluoromethoxy)phenylsulfonamido) acetate (1.15 g, 2.28 mmol) was dissolved in THF (5 mL) and MeOH (5 mL). A solution of aqueous NaOH (1 N, 3 mL) was added. The mixture was heated at 90 °C for 20 min. The solution was then allowed to cool, acidified with dilute HCl (0.1 N) until acidic by pH paper and the product partitioned into ethyl acetate. The organic portion was washed with dilute HCl (0.1 N),dried over sodium sulfate,filtered and concentrated under vacuum to give 2-(*N*-(1-(4-bromophenyl)cyclobutyl)-4-(difluoromethoxy)phenylsulfonamido)acetic acid as a light yellow-colored, semi-solid, (1.05 g, 94%).

^{1}H NMR (500 MHz, $CDCl_3$) δ ppm 1.63 (d, J = 10.68 Hz, 1H), 1.84 (dd, J = 9.31, 1.68 Hz, 1H), 2.57–2.72 (m, 2H), 2.76–2.92 (m, 2H), 4.09 (s, 2H), 6.57 (t, J = 75 Hz (C-F), 1H), 7.02 (m, J = 8.85 Hz, 2H), 7.27–7.31 (m, 2H), 7.41–7.46 (m, 2H), 7.47 (m, 2H). LC/MS 1.0 min, M−1: 489.9, Exact Mass: 491.0. HRMS Calcd for $C_{19}H_{17}O_5NBrF_2S$: 487.9973. Found: 487.9974.

The 2-(*N*-(1-(4-bromophenyl)cyclobutyl)-4-(difluoromethoxy) phenylsulfonamido)acetic acid (40 mg, 0.082 mmol) was dissolve in 1 mL of dimethylformamide. To this solution was added 2,4-dichlorophenylboronic acid (31.1 mg, 0.163 mmol), followed by sodium carbonate (15.13 mg, 0.143 mmol)and palladium(II) acetate (3.66 mg, 0.016 mmol). The mixture was placed under argon and heated at 120 °C in a microwave reactor for 20 min. LC/MS showed the reaction was ~40% complete. The mixture was filtered and purified using reverse phase HPLC employing gradient of acetonitrile in water with 0.1% TFA on a Xterra™ 30 mm × 100 mm column. The fractions containing product were combined and the solvent was removed in vacuo to obtain **12** as a light gray solid.

^{1}H NMR (500 MHz, $CDCl_3$) δ 7.57–7.48 (m, 5H), 7.39–7.32 (m, 3H), 7.28–7.26 (m, 1H), 7.06 (d, J = 8.5 Hz, 2H), 6.71–6.34 (m, 1H), 4.13 (s, 2H), 2.87 (d, J = 10.4 Hz, 2H), 2.67 (t, J = 8.7 Hz, 2H), 1.93–1.82 (m, 1H), 1.76–1.62 (m, 1H). LC/MS 1. 2 min, M−1: 554.0, Exact Mass: 555.0.

5.1.7. 2-(*N*-(1-(3′,5′-Dichlorobiphenyl-3-yl)cyclobutyl)-4-(difluoromethoxy) phenylsulfonamido)acetic acid (13)

Prepared from 1-(3-bromophenyl)cyclobutanamine in the same manner as compound **12**.

^{1}H NMR (400 MHz, CD_3OD) δ ppm 1.58–1.69 (m, 1H) 1.78–1.88 (m, 1H) 2.56–2.65 (m, 2H) 2.97–3.08 (m, 2H) 4.18 (s, 2H) 6.69 (t, J = 75.00 Hz, 1H) 6.90–6.99 (m, 2H) 7.38–7.44 (m, 5H) 7.44–7.49 (m, 2H) 7.59 (t, J = 1.76 Hz, 1H) 7.64 (dd, J = 7.65, 1.38 Hz, 1H). LC/MS 1.6 min, M−1: 554.0, Exact Mass: 555.0.

5.1.8. 2-(4-(Difluoromethoxy)-*N*-((2′-(trifluoromethoxy)-[1,1′-biphenyl]-4-yl)methyl) phenylsulfonamido)acetic acid (14)

Prepared using 4-(difluoromethoxy)benzene-1-sulfonyl chloride in the same manner as compound **26**.

^{1}H NMR (500 MHz, $CDCl_3$) δ ppm 3.96 (s, 2H), 4.47(s, 2H), 6.58 (t, J = 75 Hz (–CHF_2), 1H), 7.12 (m, J = 8.6 Hz, 2H) 7.20 (d, J = 7.9 Hz, 2H) 7.35 (d, J = 8.2 Hz, 2H) 7.35–7.40 (m, 4H) 7.75 (m, 2H) 9.88 (br. s, 1H). LC/MS 1.1 min, M−1: 556.0, Exact Mass: 557.1.

5.1.9. 2-(4-(Difluoromethoxy)-*N*-(1-(2′-(trifluoromethoxy) biphenyl-4-yl)cyclopropyl)phenylsulfonamido)acetic acid (15)

Prepared using 1-(4-bromophenyl)cyclopropanamine and (2-(trifluoromethoxy)phenyl)boronic acid in the same manner as compound **9**.

^{1}H NMR (500 MHz, $CDCl_3$) δ ppm 1.31 (br s, 2H) 1.71 (br s, 2H) 4.39 (s, 2H) 6.56 (t, J = 75.00 Hz (C-F), 1H) 7.13 (m, J = 8.55 Hz, 2H) 7.21 (d, J = 7.93 Hz, 2H) 7.35 (d, J = 8.24 Hz, 2H) 7.37–7.42 (m, 4H) 7.77 (m, 2H) 9.88 (br s, 1H). LC/MS 1.1 min, M−1: 556.0, Exact Mass: 557.1.

5.1.10. 2-(4-(Difluoromethoxy)-*N*-(1-(2′-(trifluoromethoxy) biphenyl-4-yl)cyclobutyl) phenylsulfonamido)acetic acid (16)

Prepared using 1-(4-bromophenyl)cyclobutanamine and (2-(trifluoromethoxy)phenyl)boronic acid in the same manner as compound **9**.

^{1}H NMR (500 MHz, $CDCl_3$) δ ppm 1.66–1.75 (m, 1H) 1.84–1.92 (m, 1H) 2.58–2.72 (m, 2H) 2.87 (dt, J = 11.67, 9.88 Hz, 2H) 4.13 (s, 2H) 6.51 (t, J = 75.00 Hz, 1H) 7.04 (d, J = 8.85 Hz, 2H) 7.38–7.45 (m, 6H) 7.51–7.55 (m, 4H). ^{1}H NMR (500 MHz, DMSO-d_6) δ ppm 1.74 (m, 1H) 1.99 (m, 1H) 2.46 (m, 2H) 2.53–2.63 (m, 2H) 3.54 (m, 2H) 6.96–7.14 (m, 1H) 7.31–7.59 (m, 9H) 7.85 (d, J = 8.55 Hz, 2H). LC/MS 1.1 min, M−1: 570.0, Exact Mass: 571.1. HRMS Calcd for $C_{26}H_{21}O_6NF_5S$: 570.1004. Found: 570.1004.

5.1.11. 2-(*N*-(1-(3′,5′-Dichlorobiphenyl-3-yl)cyclobutyl) phenylsulfonamido)acetic acid (17)

Prepared using 1-(3-bromophenyl)cyclobutanamine, benzene sulfonylchloride and (3,5-dichlorophenyl)boronic acid in the same manner as compound **9**.

^{1}H NMR (500 MHz, $CDCl_3$) δ ppm 1.62–1.70 (m, J = 10.60, 10.60, 7.78, 2.75 Hz, 1H) 1.82–1.90 (m, 1H) 2.59–2.67 (m, 2H) 2.85–2.94 (m, 2H) 4.17 (s, 2H) 7.27 (d, J = 2.14 Hz, 2H) 7.31–7.38 (m, 3H) 7.39–7.50 (m, 4H) 7.52–7.59 (m, 3H). LC/MS 1.5 min, M−1: 488.2, Exact Mass: 489.1. HRMS Calcd for $C_{24}H_{18}O_5NCl_2F_2S$: 540.0245. Found: 540.0246.

5.1.12. 2-(2-Chloro-*N*-(1-(3′,5′-dichlorobiphenyl-3-yl)cyclobutyl) phenylsulfonamido) acetic acid (18)

Prepared using 1-(3-bromophenyl)cyclobutanamine, 2-chlorobenzene sulfonylchloride and (3,5-dichlorophenyl)boronic acid in the same manner as compound **9**.

^{1}H NMR (500 MHz, $CDCl_3$) δ ppm 1.51–1.58 (m, 1H) 1.73–1.80 (m, 1H) 2.53–2.60 (m, 2H) 2.91–2.98 (m, 2H) 4.47 (s, 2H) 7.15–7.22 (m, 1H) 7.29–7.38 (m, 7H) 7.49–7.55 (m, 2H) 7.83 (dd, J = 8.09, 1.37 Hz, 1H). LC/MS 1.6 min, M−1: 525.0, Exact Mass: 523.0. HRMS Calcd for $C_{24}H_{19}O_4NCl_3S$: 522.0095. Found: 522.0098.

5.1.13. 2-(3-Chloro-*N*-(1-(3′,5′-dichlorobiphenyl-3-yl)cyclobutyl)phenylsulfonamido) acetic acid (19)

Prepared using 1-(3-bromophenyl)cyclobutanamine, 3-chlorobenzene sulfonylchloride and (3,5-dichlorophenyl)boronic acid in the same manner as compound **9**.

^{1}H NMR (500 MHz, $CDCl_3$) δ ppm 1.64–1.72 (m, 1H) 1.89 (m, 1H) 2.63–2.69 (m, 2H) 2.84–2.92 (m, 2H) 4.25 (s, 2H) 7.23–7.28 (m, 2H) 7.28–7.31 (m, 2H) 7.34–7.38 (m, 2H) 7.39–7.47 (m, 3H) 7.48–7.50 (m, 1H) 7.53–7.56 (m, 1H). LC/MS 1.6 min, M−1: 525.0, Exact Mass: 523.0. HRMS Calcd for $C_{24}H_{19}O_4NCl_3S$: 522.0095. Found: 522.0098.

5.1.14. 2-(4-Chloro-*N*-(1-(3′,5′-dichlorobiphenyl-3-yl)cyclobutyl)phenylsulfonamido) acetic acid (20)

Prepared using 1-(3-bromophenyl)cyclobutanamine, 4-chlorobenzene sulfonylchloride and (3,5-dichlorophenyl)boronic acid in the same manner as compound **9**.

^{1}H NMR (500 MHz, $CDCl_3$) δ ppm 1.63–1.71 (m, 1H) 1.87 (m, 1H) 2.60–2.66 (m, 2H) 2.83–2.91 (m, 2H) 4.22 (s, 2H) 7.23–7.27 (m, 2H) 7.27–7.30 (m, 2H) 7.38 (t, J = 1.83 Hz, 1H) 7.40–7.46 (m, 4H) 7.47–7.49 (m, 1H) 7.54–7.59 (m, 1H). LC/MS 1.6 min, M−1: 525.0, Exact Mass: 523.0. HRMS Calcd for $C_{24}H_{19}O_4NCl_3S$: 522.0095. Found: 522.0098.

5.1.15. 2-(4-Cyano-*N*-(1-(3′,5′-dichlorobiphenyl-3-yl)cyclobutyl) phenylsulfonamido) acetic acid (21)

Prepared using 1-(3-bromophenyl)cyclobutanamine, 4-cyanobenzene sulfonylchloride and (3,5-dichlorophenyl)boronic acid in the same manner as compound **9**.

^{1}H NMR (500 MHz, $CDCl_3$) δ ppm 1.67 (dd, J = 7.78, 2.90 Hz, 1H) 1.83–1.90 (m, 1H) 2.58–2.68 (m, 2H) 2.80–2.89 (m, 2H) 4.29 (s, 2H) 7.30 (d, J = 1.83 Hz, 2H) 7.38–7.42 (m, 2H) 7.45 (d, J = 7.93 Hz, 1H) 7.52–7.56 (m, 2H) 7.58 (m, 2H) 7.63 (m, 2H). LC/MS 2.1 min, M−1: 513.2, Exact Mass: 514.1. HRMS Calcd for $C_{25}H_{19}O_4N_2Cl_2S$: 513.0437. Found: 513.0436.

5.1.16. 2-(*N*-(1-(3′,5′-Dichlorobiphenyl-3-yl)cyclobutyl)-3-methoxyphenylsulfonamido) acetic acid (22)

Prepared using 1-(3-bromophenyl)cyclobutanamine, 3-methoxy benzene sulfonyl chloride and (3,5-dichlorophenyl)boronic acid in the same manner as compound **9**.

^{1}H NMR (500 MHz, $CDCl_3$) δ ppm 1.62–1.69 (m, 1H) 1.86 (q, J = 9.36 Hz, 1H) 2.63 (t, J = 8.85 Hz, 2H) 2.89 (dd, J = 10.22, 2.59 Hz, 2H) 3.72 (s, 3H) 4.20 (s, 2H) 6.96 (dd, J = 7.78, 1.98 Hz, 1H) 7.02–7.04 (m, 1H) 7.17 (d, J = 8.54 Hz, 1H) 7.25 (t, J = 7.93 Hz, 1H) 7.37 (t, J = 1.83 Hz, 1H) 7.39–7.43 (m, 2H) 7.48 (s, 2H) 7.57 (d, J = 6.41 Hz, 1H). LC/MS 1.7 min, M−1: 518.2, Exact Mass: 519.1. HRMS Calcd for $C_{25}H_{23}O_5NCl_2NaS$: 542.0566. Found: 542.0563.

5.1.17. 2-(*N*-(1-(3′,5′-Dichlorobiphenyl-3-yl)cyclobutyl)-2-methoxyphenylsulfonamido) acetic acid (23)

Prepared using 1-(3-bromophenyl)cyclobutanamine, 2-methoxy benzene sulfonyl chloride and (3,5-dichlorophenyl)boronic acid in the same manner as compound **9**.

^{1}H NMR (500 MHz, $CDCl_3$) δ ppm 1.50–1.60 (m, 1H) 1.70–1.82 (m, 1H) 2.54–2.63 (m, 2H) 2.81–2.90 (m, 2H) 3.83 (s, 3H) 4.43 (s, 2H) 6.80 (d, J = 8.54 Hz, 1H) 6.83 (t, J = 7.63 Hz, 1H) 7.28–7.31 (m, 4H) 7.32–7.35 (m, 1H) 7.36 (t, J = 1.83 Hz, 1H) 7.48–7.53 (m, 2H) 7.60 (dd, J = 7.93, 1.53 Hz, 1H). LC/MS 1.7 min, M−1: 518.2, Exact Mass: 519.1. HRMS Calcd for $C_{25}H_{23}O_5NCl_2NaS$: 542.0566. Found: 542.0563.

5.1.18. 2-(*N*-(1-(3′,5′-Dichlorobiphenyl-3-yl)cyclobutyl)-2,2-dimethylchroman-6-sulfonamido)acetic acid (24)

Prepared using 1-(3-bromophenyl)cyclobutanamine, 2,2-dimethylchromane-6-sulfonyl chloride and (3,5-dichlorophenyl) boronic acid in the same manner as compound **9**.

^{1}H NMR (500 MHz, $CDCl_3$) δ ppm 1.26 (s, 6H) 1.67 (t, J = 6.71 Hz, 3H) 1.85–1.94 (m, 1H) 2.53 (t, J = 6.56 Hz, 2H) 2.67 (t, J = 8.85 Hz, 2H) 2.83–2.92 (m, 2H) 4.14 (s, 2H) 6.68 (d, J = 8.85 Hz, 1H) 6.89 (d, J = 1.83 Hz, 1H) 7.23–7.27 (m, 3H) 7.36 (t, J = 1.83 Hz, 1H) 7.43–7.48 (m, 2H) 7.49 (s, 1H) 7.60 (dd, J = 5.49, 2.44 Hz, 1H). ^{13}C NMR (101 MHz, chloroform-d) δ 173.2, 157.9, 143.8, 143.4, 138.7, 135.4, 130.4, 129.2, 128.8, 127.3, 127.0, 126.9, 126.3, 126.1, 125.6, 121.0, 117.4, 75.6, 65.8, 48.3, 35.2, 32.1, 26.8, 22.2, 14.7. LC/MS 1.7 min, M−1: 572.1, Exact Mass: 573.1. HRMS Calcd for $C_{29}H_{30}O_5NCl_2S$: 574.1216. Found: 574.1206.

5.1.19. 2-(*N*-((3′,5′-Dichloro-[1,1′-biphenyl]-3-yl)methyl)-2,2-dimethylchroman-6-sulfonamido)acetic acid (25)

Prepared from 1-bromo-3-(bromomethyl)benzene in the same manner as compound **26**.

^{1}H NMR (500 MHz, CDCl3) δ 7.61–7.57 (m, 2H), 7.44 (d, J = 7.8 Hz, 1H), 7.39 (d, J = 7.6 Hz, 1H), 7.37 (d, J = 1.8 Hz, 2H), 7.34 (s, 1H), 7.32 (t, J = 1.8 Hz, 1H), 7.26 (d, J = 7.0 Hz, 1H), 6.87–6.83 (m, 1H), 4.51 (s, 2H), 3.95 (s, 2H), 2.77 (t, J = 6.7 Hz, 2H), 1.79 (t, J = 6.7 Hz, 2H), 1.32 (s, 6H). LC/MS 2.5 min, M−1: 532.2, Exact Mass: 533.1.

5.1.20. 2-(*N*-((3′,5′-Dichloro-[1,1′-biphenyl]-4-yl)methyl)-2,2-dimethylchroman-6-sulfonamido)acetic acid (26)

To a −30 °C solution of 2,2-dimethylchroman-6-sulfonyl chloride (3.165 g, 10.92 mmol) in dichloromethane (50 mL) was added *tert*-butyl 2-aminoacetate (2.308 mL, 16.39 mmol), Hunig's base (3.82 mL, 21.85 mmol) and a catalytic amount of DMAP. The orange–red colored mixture was stirred at 25 °C overnight and slowly turned bright yellow. The crude reaction mixture was diluted with ethyl acetate and sequentially extracted with HCl (aq), $NaHCO_3$ (aq) and brine. The organic portion was dried over $MgSO_4$ and the solvent removed to leave a white powder. After drying under vacuum overnight, *tert*-butyl 2-(2,2-dimethylchroman-6-sulfonamido)acetate (3.6 g, 9.62 mmol, 88% yield) was isolated in sufficient purity to use directly in the next step with no further purification.

^{1}H NMR (500 MHz, $CDCl_3$) δ 7.62–7.48 (m, 2H), 6.83 (d, J = 8.5 Hz, 1H), 3.64 (d, J = 5.2 Hz, 2H), 2.81 (t, J = 6.7 Hz, 2H), 1.81 (t, J = 6.9 Hz, 2H), 1.35 (s, 9H), 1.34 (s, 6H)

To a solution of *tert*-butyl 2-(2,2-dimethylchroman-6-sulfonamido)acetate (500 mg, 1.407 mmol) in acetonitrile (15 mL) was added BEMP-resin (786 mg, 1.547 mmol) followed by 1-bromo-4-(bromomethyl)benzene (602 mg, 2.409 mmol). The mixture was heated in microwave reactor at 90 °C for 3 h. The resin was removed by filtration and rinsed alternately with dichloromethane and methanol. The combined organic portions were concentrated by rotary evaporation to give an orange red residue. The residue was dissolved in hexanes and a minimum amount of dichloromethane, charged to a silica-column and chromatographed using a gradient of 10–20% ethyl acetate in hexanes over 3 column volumes. The fractions containing the product were combined and the solvent was removed to obtain clear oil. The oil solidified whiling drying under high vacuum overnight to provide *tert*-butyl 2-(*N*-(4-bromobenzyl)-2,2-dimethylchroman-6-sulfonamido)acetate (632 mg, 1.205 mmol, 86% yield) as a white solid.

^{1}H NMR (500 MHz, $CDCl_3$) δ 7.56 (s, 2H), 7.43 (d, J = 8.2 Hz, 2H), 7.14 (d, J = 8.5 Hz, 2H), 6.89–6.81 (m, 1H), 4.45 (s, 2H), 3.78 (s, 2H), 2.79 (s, 2H), 1.83 (t, J = 6.7 Hz, 2H), 1.39–1.28 (m, 15H).

The final compounds were obtained using parallel synthesis techniques as follows:

A series of $ArB(OH)_2$ (0.210 mmol) were individually weighed into separate reaction vials. To each tube was added an aqueous solution of K_3PO_4 (0.140 mL, 0.280 mmol). A dimethylformamide (1.5 mL) solution of *tert*-butyl 2-(*N*-(4-bromobenzyl)-2,2-dimethylchroman-6-sulfonamido)acetate (36.7 mg, 0.070 mmol) was distributed to each reaction tube, followed by $Pd(Ph_3P)_4$ (8.09 mg, 7.00 μmol (amount estimated without weighing)). The reaction vial was immediately sealed under nitrogen and heated in an oil bath at 100–105 °C overnight. The crude reaction mixture was filtered through a 0.45 μm PVDF to give a clear solution which was purified by direct injection onto a preparative HPLC and eluted with an 50–100% step-gradient of acetonitrile in a water 0.1% TFA buffer system. The fractions containing the desired product were combined and the solvent removed in vacuo. To hydrolyze the *tert*-butyl ester, the residue was dissolved in dichloromethane (2 mL) and TFA (1 mL) and then stirred at room temperature for 1 hour. The solvent was removed under vacuum. The crude reaction mixture was filtered through a 0.45 μm PVDF to give a clear solution which was purified by direct injection onto a preparative HPLC and eluted with a 40–100% step-gradient of acetonitrile in a water 0.1%TFA buffer system. The fractions containing the desired product were combined and the solvent removed in vacuo. The purified compounds were dried under high vacuum overnight.

^{1}H NMR (500 MHz, $CDCl_3$) δ 7.62–7.57 (m, 2H), 7.46 (d, J = 8.2 Hz, 2H), 7.41 (d, J = 1.8 Hz, 2H), 7.33 (t, J = 1.8 Hz, 1H), 7.31 (d, J = 8.2 Hz, 2H), 6.85 (d, J = 8.5 Hz, 1H), 4.48 (s, 2H), 3.95 (s, 2H), 2.80 (t, J = 6.7 Hz, 2H), 1.83 (t, J = 6.7 Hz, 2H), 1.35 (s, 6H). LC/MS 2.5 min, M−1: 532.2, Exact Mass: 533.1.

5.1.21. 2-(*N*-(1-(3′,5′-Dichlorobiphenyl-3-yl)cyclopentyl)-2,2-dimethylchroman-6-sulfonamido)acetic acid (27)

Prepared using 1-(3-bromophenyl)cyclopentanamine, 2,2-dimethylchromane-6-sulfonyl chloride and (3,5-dichlorophenyl) boronic acid in the same manner as compound **9**.

^{1}H NMR (500 MHz, CD_3OD) δ ppm 1.28 (s, 6H) 1.69 (t, J = 6.71 Hz, 2H) 2.35–2.42 (m, 2H) 2.50–2.65 (m, 4H) 2.74–2.80 (m, 2H) 2.88 (t, J = 6.87 Hz, 2H) 4.33 (s, 2H) 6.61 (d, J = 8.85 Hz, 1H) 7.08 (d, J = 2.14 Hz, 1H) 7.29 (dd, J = 8.55, 2.44 Hz, 1H) 7.45 (m, 4H) 7.59 (d, J = 3.05 Hz, 1H) 7.61 (m, 2H). LC/MS 1.9 min, M−1: 586.3, Exact Mass: 587.1.

5.1.22. 2-(*N*-(3-(3′,5′-Dichlorobiphenyl-4-yl)tetrahydrofuran-3-yl)-2,2-dimethylchroman-6-sulfonamido) acetic acid (28)

Prepared using 3-(4-bromophenyl)tetrahydrofuran-3-amine, 2,2-dimethylchromane-6-sulfonyl chloride and (3,5-dichlorophenyl)boronic acid in the same manner as compound **9**.

^{1}H NMR (500 MHz, $CDCl_3$) δ ppm 1.39 (s, 6H) 1.87 (t, J = 6.71 Hz, 2H) 2.31–2.45 (m, 2H) 2.82–2.90 (m, 1H) 2.90–2.97 (m, 1H) 3.51–3.63 (m, 1H) 4.02–4.07 (m, 1H) 4.35 (q, J = 18.31 Hz, 2H) 4.46 (d, J = 9.46 Hz, 1H) 4.64 (d, J = 9.46 Hz, 1H) 6.53 (d, J = 8.55 Hz, 1H) 6.91 (d, J = 8.55 Hz, 1H) 7.00 (s, 1H) 7.16 (dd, J = 8.70, 1.98 Hz, 1H) 7.32–7.39 (m, 2H) 7.41 (d, J = 1.83 Hz, 2H) 7.62–7.72 (m, 2H). LC/MS 1.6 min, M−1: 588.2, Exact Mass: 589.1.

5.1.23. 2-(*N*-([1,1′-Biphenyl]-3-ylmethyl)-2,2-dimethylchroman-6-sulfonamido)acetic acid (29)

Prepared using 3-(bromomethyl)-1,1′-biphenyl and 2,2-dimethylchromane-6-sulfonyl chloride in the same manner as compound **5**.

^{1}H NMR (500 MHz, $CDCl_3$) δ 7.61 (d, J = 6.3 Hz, 1H), 7.60 (s, 1H), 7.51 (d, 1H), 7.50 (d, J = 7.4 Hz, 2H), 7.41 (dd, J = 13.4, 5.5 Hz, 2H), 7.39 (s, 1H), 7.36 (d, J = 7.7 Hz, 1H), 7.34 (t, J = 7.3 Hz, 1H), 7.19 (d, J = 7.6 Hz, 1H), 6.87–6.83 (m, 1H), 4.52 (s, 2H), 3.97 (s, 2H), 2.77 (t, J = 6.7 Hz, 2H), 1.79 (t, J = 6.7 Hz, 2H), 1.33 (s, 6H). LC/MS 1.4 min, M−1: 464.3, Exact Mass: 465.2.

5.1.24. 2-(2,2-Dimethyl-*N*-(quinolin-8-ylmethyl)chroman-6-sulfonamido)acetic acid (30)

Prepared using 8-(bromomethyl)quinoline and 2,2-dimethylchromane-6-sulfonyl chloride in the same manner as compound **5**.

^{1}H NMR (600 MHz, DMSO/$CDCl_3$) δ 8.85–8.81 (m, 1H), 8.29 (d, J = 8.2 Hz, 1H), 7.85 (d, J = 8.2 Hz, 1H), 7.70 (d, J = 7.0 Hz, 1H), 7.52 (d, J = 7.6 Hz, 1H), 7.51–7.47 (m, 1H), 7.42–7.37 (m, 2H), 6.69 (d, J = 8.2 Hz, 1H), 5.03 (s, 2H), 4.06 (s, 2H), 2.67 (t, J = 6.7 Hz, 2H), 1.76 (t, J = 6.7 Hz, 2H), 1.29 (s, 6H). LC/MS 3.4 min, M−1: 497.6, Exact Mass: 498.1. HRMS Calcd for $C_{23}H_{25}O_5N_2S$: 441.1479. Found: 441.1466.

5.1.25. (*R*)-2-(4-(Difluoromethoxy)-*N*-(1-phenylethyl) phenylsulfonamido)acetic acid (31)

Prepared using (*R*)-1-phenylethan-1-amine and 4-(difluoromethoxy)benzene-1-sulfonyl chloride in the same manner as compound **9**.

^{1}H NMR (500 MHz, chloroform-*d*) δ ppm 1.46 (d, J = 7.02 Hz, 3H) 3.73 (d, J = 18.31 Hz, 1H) 4.01 (d, J = 18.62 Hz, 1H) 5.10 (q, J = 7.02 Hz, 1H) 6.61 (t, J = 75 Hz (H-F), 1H) 7.15 (br s, 1H) 7.16 (d, J = 2.44 Hz, 1H) 7.19–7.36 (m, 5H) 7.96 (d, J = 8.85 Hz, 2H). LC/MS 0.8 min, M−1: 384.3, Exact Mass: 385.1.

5.1.26. 2-(*N*-((2′,3′-Dichloro-[1,1′-biphenyl]-3-yl)methyl)-4-(difluoromethoxy) phenylsulfonamido)acetic acid (32)

Prepared using 4-(Difluoromethoxy)benzene-1-sulfonyl chloride, 1-bromo-4-(bromomethyl)benzene and (2,3-dichlorophenyl) boronic acid in the same manner as compound **26**.

^{1}H NMR (400 MHz, $CDCl_3$) δ 7.93 (d, J = 8.8 Hz, 2H), 7.52–7.46 (m, 1H), 7.45–7.38 (m, 1H), 7.38–7.33 (m, 1H), 7.32–7.30 (m, 1H), 7.27–7.21 (m, 4H), 7.20–7.15 (m, 1H), 6.60 (t, J = 72.6 Hz, 1H), 4.59 (s, 2H), 4.04 (s, 2H). LC/MS 3.9 min, M−1: 514.5, Exact Mass: 515.0. HRMS Calcd for $C_{22}H_{16}O_5NCl_2F_2S$: 514.0089. Found: 514.0089.

5.1.27. 2-(4-(Difluoromethoxy)-*N*-((2′-(trifluoromethoxy)-[1,1′-biphenyl]-3-yl)methyl) phenylsulfonamido)acetic acid (33)

Prepared using 4-(Difluoromethoxy)benzene-1-sulfonyl chloride, 1-bromo-3-(bromomethyl)benzene and (2-trifluoromethoxyphenyl)boronic acid in the same manner as compound **26**.

^{1}H NMR (600 MHz, DMSO/$CDCl_3$) δ 7.91 (d, J = 8.2 Hz, 2H), 7.51–7.35 (m, 6H), 7.32–7.24 (m, 4H), 4.51 (s, 2H), 3.89–3.79 (m, 2H) LC/MS 4.0 min, M−1: 530.6, Exact Mass: 531.1.

5.1.28. 2-(3,4-Dichloro-*N*-(1-(2′,4′-dichloro-[1,1′-biphenyl]-3-yl)cyclobutyl) phenylsulfonamido)acetic acid (34)

Prepared using 3,4-dichlorobenzene-1-sulfonyl chloride, 1-bromo-3-(bromomethyl)benzene and (2,4-dichlorophenyl)boronic acid in the same manner as compound **26**.

^{1}H NMR (500 MHz, $CDCl_3$) δ ppm 1.65–1.73 (m, 1H) 1.88 (d, J = 10.68 Hz, 1H) 2.66 (t, J = 8.85 Hz, 2H) 2.82–2.92 (m, 2H) 4.18 (s, 2H) 7.19 (d, J = 8.24 Hz, 1H) 7.33–7.42 (m, 5H) 7.46 (d, J = 1.22 Hz, 1H) 7.47–7.53 (m, 3H). ESI-MS m/z 560 (MH^+).

Supplementary data

Supplementary data associated with this article can be found, in the online version, at http://dx.doi.org/10.1016/j.bmc.2016.02.006.

References and notes

1. Pacher, P.; Kunos, G. *FEBS J.* **1918**, *2013*, 280.
2. Gunduz-Cinar, O.; Hill, M. N.; McEwen, B. S.; Holmes, A. *Trends Pharmacol. Sci.* **2013**, *34*, 637.
3. Hillard, C. J.; Liu, Q.-S. *Curr. Pharm. Des.* **2014**, *20*, 3795.
4. Maione, S.; Costa, B.; Di Marzo, V. *Pain* **2013**, *154*, S87.
5. Kohnz, R. A.; Nomura, D. K. *Chem. Soc. Rev.* **2014**, *43*, 6859.
6. Ruby, M. A.; Nomura, D. K.; Hudak, C. S. S.; Barber, A.; Casida, J. E.; Krauss, R. M. *PLoS One* **2011**, *6*, e26415.
7. Di Marzo, V. *Nat. Neurosci.* **2011**, *14*, 9.
8. Di Marzo, V. *Pharmacol. Res.* **2009**, *60*, 77.
9. Nicoll Roger, A.; Alger Bradley, E. *Sci. Am.* **2004**, *291*, 68.
10. Storr, M. A.; Sharkey, K. A. *Curr. Opin. Pharmacol.* **2007**, *7*, 575.
11. Kunos, G.; Osei-Hyiaman, D.; Liu, J.; Godlewski, G.; Batkai, S. *J. Biol. Chem.* **2008**, *283*, 33021.
12. Sharkey, K. A.; Darmani, N. A.; Parker, L. A. *Eur. J. Pharmacol.* **2014**, *722*, 134.
13. Davis, M. P. *Expert Opin. Invest. Drugs* **2008**, *17*, 85.
14. Moreira, F. A.; Grieb, M.; Lutz, B. *Best Pract. Res., Clin. Endocrinol. Metab.* **2009**, *23*, 133.
15. Muccioli, G. G. *Drug Discovery Today* **2010**, *15*, 474.
16. Hu, S.; Huang, Y.; Ding, M.; Chupak, L. S.; Zheng, X.; Gentles, R. G. *Preparation of Glycine Chroman-6-sulfonamides for Use as Inhibitors of Diacylglycerol Lipase*; Bristol-Myers Squibb Company: USA, 2011. p 98.
17. Chupak, L. S.; Zheng, X.; Ding, M.; Hu, S.; Huang, Y.; Gentles, R. G. *Preparation of Glycine Sulfonamides for Use as Inhibitors of Diacylglycerol Lipase*; Bristol-Myers Squibb Company: USA, 2011. p 62.
18. Ahn, K.; McKinney, M. K.; Cravatt, B. F. *Chem. Rev.* **2008**, *108*, 1687.
19. Ezzili, C.; Otrubova, K.; Boger, D. L. *Bioorg. Med. Chem. Lett.* **2010**, *20*, 5959.
20. Ueda, N.; Tsuboi, K.; Uyama, T.; Ohnishi, T. *BioFactors* **2010**, *37*, 1.
21. Tanimura, A.; Yamazaki, M.; Hashimotodani, Y.; Uchigashima, M.; Kawata, S.; Abe, M.; Kita, Y.; Hashimoto, K.; Shimizu, T.; Watanabe, M.; Sakimura, K.; Kano, M. *Neuron* **2010**, *65*, 320.
22. Gao, Y.; Vasilyev, D. V.; Goncalves, M. B.; Howell, F. V.; Hobbs, C.; Reisenberg, M.; Shen, R.; Zhang, M. Y.; Strassle, B. W.; Lu, P.; Mark, L.; Piesla, M. J.; Deng, K.; Kouranova, E. V.; Ring, R. H.; Whiteside, G. T.; Bates, B.; Walsh, F. S.; Williams, G.; Pangalos, M. N.; Samad, T. A.; Doherty, P. *J. Neurosci.* **2017**, *2010*, 30.
23. Reisenberg, M.; Singh, P. K.; Williams, G.; Doherty, P. *Philos. Trans. R. Soc. Lond. B Biol. Sci.* **2012**, *367*, 3264.
24. Bisogno, T.; Howell, F.; Williams, G.; Minassi, A.; Grazia Cascio, M.; Ligresti, A.; Matias, I.; Schiano-Moriello, A.; Paul, P.; Williams, E.-J.; Gangadharan, U.; Hobbs, C.; Di Marzo, V.; Doherty, P. *J. Cell Biol.* **2003**, *163*, 463.

25. Suarez, J.; Bermudez-Silva, F. J.; Mackie, K.; Ledent, C.; Zimmer, A.; Cravatt, B. F.; De, F. F. R. *J. Comp. Neurol.* **2008**, *509*, 400.
26. Yoshida, T.; Fukaya, M.; Uchigashima, M.; Miura, E.; Kamiya, H.; Kano, M.; Watanabe, M. *J. Neurosci.* **2006**, *26*, 4740.
27. Lafourcade, M.; Elezgarai, I.; Mato, S.; Bakiri, Y.; Grandes, P.; Manzoni, O. J. *PloS One* **2007**, 2.
28. Uchigashima, M.; Narushima, M.; Fukaya, M.; Katona, I.; Kano, M.; Watanabe, M. *J. Neurosci.* **2007**, *27*, 3663.
29. Di Marzo, V. *Nat. Rev. Drug Disc.* **2008**, *7*, 438.
30. Pacher, P.; BÃ¡tkai, S.; Kunos, G. *Pharmacol. Rev.* **2006**, *58*, 389.
31. Di Marzo, V. *Pharmacol. Res.* **2009**, *60*, 77.
32. Kunos, G.; Tam, J. *Br. J. Pharmacol.* **2011**, *163*, 1423.
33. Bisogno, T.; Cascio, M. G.; Saha, B.; Mahadevan, A.; Urbani, P.; Minassi, A.; Appendino, G.; Saturnino, C.; Martin, B.; Razdan, R.; Di Marzo, V. *Biochim. Biophys. Acta, Mol. Cell Biol. Lipids* **2006**, *1761*, 205.
34. Hoover, H. S.; Blankman, J. L.; Niessen, S.; Cravatt, B. F. *Bioorg. Med. Chem. Lett.* **2008**, *18*, 5838.
35. Bisogno, T.; Burston, J. J.; Rai, R.; Allara, M.; Saha, B.; Mahadevan, A.; Razdan, R. K.; Wiley, J. L.; Di Marzo, V. *ChemMedChem* **2009**, *4*, 946.
36. Janssen, F. J.; Deng, H.; Baggelaar, M. P.; Allara, M.; van der Wel, T.; den Dulk, H.; Ligresti, A.; van Esbroeck, A. C.; McGuire, R.; Di Marzo, V.; Overkleeft, H. S.; van der Stelt, M. *J. Med. Chem.* **2014**, *57*, 6610.
37. Anonymous Report on carcinogens : carcinogen profiles/U.S. Dept. of Health and Human Services, Public Health Service, National Toxicology Program, 12, 38.
38. Birch, A. M.; Groombridge, S.; Law, R.; Leach, A. G.; Mee, C. D.; Schramm, C. *J. Med. Chem.* **2012**, *55*, 3923.
39. Benigni, R.; Bossa, C. *Chem. Rev.* **2011**, *111*, 2507.
40. Miyaura, N.; Suzuki, A. *Chem. Rev. (Washington, D. C.)* **1995**, *95*, 2457.
41. Pedicord, D. L.; Flynn, M. J.; Fanslau, C.; Miranda, M.; Hunihan, L.; Robertson, B. J.; Pearce, B. C.; Yu, X. C.; Westphal, R. S.; Blat, Y. *Biochem. Biophys. Res. Commun.* **2011**, *411*, 809.
42. Baggelaar, M. P.; Janssen, F. J.; van Esbroeck, A. C.; den Dulk, H.; Allara, M.; Hoogendoorn, S.; McGuire, R.; Florea, B. I.; Meeuwenoord, N.; van den Elst, H.; van der Marel, G. A.; Brouwer, J.; Di Marzo, V.; Overkleeft, H. S.; van der Stelt, M. *Angew. Chem., Int. Ed.* **2013**, *52*, 12081.
43. Nardini, M.; Dijkstra, B. W. *Curr. Opin. Struct. Biol.* **1999**, *9*, 732.
44. Kansy, M.; Senner, F.; Gubernator, K. *J. Med. Chem.* **1998**, *41*, 1007.
45. Tran, A.; Rey, E.; Pons, G.; Rousseau, M.; d'Athis, P.; Olive, G.; Mather, G. G.; Bishop, F. E.; Wurden, C. J.; Labroo, R.; Trager, W. F.; Kunze, K. L.; Thummel, K. E.; Vincent, J. C.; Gillardin, J.-M.; Lepage, F.; Levy, R. H. *Clin. Pharmacol. Ther. (St. Louis)* **1997**, *62*, 490.
46. Weaver, C. D.; Harden, D.; Dworetzky, S. I.; Robertson, B.; Knox, R. J. *J. Biomol. Screening* **2004**, *9*, 671.
47. Zvyaga, T.; Chang, S.-Y.; Chen, C.; Yang, Z.; Vuppugalla, R.; Hurley, J.; Thorndike, D.; Wagner, A.; Chimalakonda, A.; Rodrigues, A. D. *Drug Metab. Dispos.* **2012**, *40*, 1698.
48. Herbst, J.; Anthony, M.; Stewart, J.; Connors, D.; Chen, T.; Banks, M.; Petrillo, E. W.; Agler, M. *Assay Drug Dev. Technol.* **2009**, *7*, 294.

Please cite this article in press as: Chupak, L. S.; et al. *Bioorg. Med. Chem.* (2016), http://dx.doi.org/10.1016/j.bmc.2016.02.006